Pressure-induced phase transitions and superconductivity in a quasi–1-dimensional topological crystalline insulator α-Bi_4Br_4

Xiang Li[a,b,1], Dongyun Chen[a,1], Meiling Jin[c,1], Dashuai Ma[a], Yanfeng Ge[d], Jianping Sun[e], Wenhan Guo[f], Hao Sun[a], Junfeng Han[a], Wende Xiao[a], Junxi Duan[a], Qinsheng Wang[a], Cheng-Cheng Liu[a], Ruqiang Zou[f], Jinguang Cheng[e], Changqing Jin[e], Jianshi Zhou[b], John B. Goodenough[b,2], Jinlong Zhu[c,g,2], and Yugui Yao[a,h,i,2]

[a]Key Laboratory of Advanced Optoelectronic Quantum Architecture and Measurement of Ministry of Education, School of Physics, Beijing Institute of Technology, Beijing 100081, China; [b]Materials Science and Engineering Program, Mechanical Engineering Department, University of Texas at Austin, Austin, TX 78712; [c]Center for High Pressure Science and Technology Advanced Research, Beijing 100094, China; [d]State Key Laboratory of Metastable Materials Science and Technology and Key Laboratory for Microstructural Material Physics of Hebei Province, School of Science, Yanshan University, Qinhuangdao 066004, China; [e]Beijing National Laboratory for Condensed Matter Physics and Institute of Physics, Chinese Academy of Sciences, Beijing 100190, China; [f]Beijing Key Laboratory for Theory and Technology of Advanced Battery Materials, Department of Materials Science and Engineering, College of Engineering, Peking University, Beijing 100871, China [g]Physics Department, Southern University of Science and Technology, Shenzhen 518055, China; [h]Micronano Centre, Beijing Key Lab of Nanophotonics and Ultrafine Optoelectronic Systems, Beijing Institute of Technology, Beijing 100081, China; and [i]State Key Laboratory of Explosion Science and Technology, Beijing Institute of Technology, Beijing 100081, China

Contributed by John B. Goodenough, July 2, 2019 (sent for review June 3, 2019; reviewed by Alexey Taskin and Xiangang Wan)

Great progress has been achieved in the research field of topological states of matter during the past decade. Recently, a quasi–1-dimensional bismuth bromide, Bi_4Br_4, has been predicted to be a rotational symmetry-protected topological crystalline insulator; it would also exhibit more exotic topological properties under pressure. Here, we report a thorough study of phase transitions and superconductivity in a quasihydrostatically pressurized α-Bi_4Br_4 crystal by performing detailed measurements of electrical resistance, alternating current magnetic susceptibility, and in situ high-pressure single-crystal X-ray diffraction together with first principles calculations. We find a pressure-induced insulator–metal transition between ∼3.0 and 3.8 GPa where valence and conduction bands cross the Fermi level to form a set of small pockets of holes and electrons. With further increase of pressure, 2 superconductive transitions emerge. One shows a sharp resistance drop to 0 near 6.8 K at 3.8 GPa; the transition temperature gradually lowers with increasing pressure and completely vanishes above 12.0 GPa. Another transition sets in around 9.0 K at 5.5 GPa and persists up to the highest pressure of 45.0 GPa studied in this work. Intriguingly, we find that the first superconducting phase might coexist with a nontrivial rotational symmetry-protected topology in the pressure range of ∼3.8 to 4.3 GPa; the second one is associated with a structural phase transition from monoclinic *C2/m* to triclinic *P*-1 symmetry.

topological materials | superconductivity | high pressure | quasi–1-dimensional bismuth bromide

Symmetry-protected topological materials have attracted considerable attention ever since the discovery of Z_2-type topological insulators (1–4). Among them, topological crystalline insulators (TCIs) and topological superconductors are mostly known in 2-dimensional (2D) and 3-dimensional topological phases (5–8). The search for topological superconductivity in TCIs is currently an active research endeavor in condensed matter physics (9–11). Recent theoretical works have proposed that quasi–1-dimensional (quasi-1D) α-Bi_4Br_4 (Fig. 1*A*) could provide an example of a rotation symmetry-protected TCI having a quite large band gap with the coexistence of 2D gapless Dirac cone surface states and 1D hinge states (12, 13). Another quasi-1D β-Bi_4Br_4 (Fig. 1*B*) having the same monoclinic *C2/m* symmetry but only half-block stacking along the *c* axis has been predicted to exhibit a Weyl semimetal phase between a weak topological insulator (WTI) and a strong topological insulator phase (14–16). These predictions have sparked interest in investigating their topological characters and electronic structures, which can be easily tuned by external pressure due to their weakly connected quasi-1D structures. Providing a clean variation without introducing chemical doping complexity, pressure can dramatically alter a quasi-1D lattice so as to lead to a possibility of induced superconductivity. A question arises naturally: is it possible to achieve superconductivity in α-Bi_4Br_4 or β-Bi_4Br_4 under high pressure while their topological states remain intact?

In fact, pressure-induced superconductivity and topological phase transitions have been experimentally observed in the sister compound Bi_4I_4 (17–19), which adopts an analogous structure consisting of 1D molecular chains that are coupled by weak van der Waals interactions. Two crystalline modifications, α-Bi_4I_4 and β-Bi_4I_4, are confirmed to be a normal insulator and a WTI at ambient pressure, respectively (20–22). Under high pressure, the β-Bi_4I_4 phase undergoes superconductive and quantum phase transitions that originate from its structural instability (18). Different from Bi_4I_4, while β-Bi_4Br_4 has not yet been identified

Significance

The quasi–1-dimensional bismuth bromide, α-Bi_4Br_4, has been predicted to be a rotational symmetry-protected topological crystalline insulator. The structural study under high pressure indicates that the α-Bi_4Br_4 phase is stable up to 4.3 GPa. There is a rich phase diagram of physical properties under high pressure in the α-Bi_4Br_4 phase (i.e., a pressure-induced insulator–metal transition and, most importantly, a superconductive phase near the boundary of the insulator–metal transition). These findings help to answer questions, such as whether it is possible for the symmetry-protected electrons to form Cooper pairs. The α-Bi_4Br_4 undergoes a pressure-induced structural transition above 4.3 GPa to a triclinic *P*-1 phase, which is another superconductive phase.

Author contributions: X.L., J.B.G., J. Zhu, and Y.Y. designed research; X.L., D.C., M.J., D.M., Y.G., J.S., W.G., and H.S. performed research; X.L., D.C., M.J., D.M., Y.G., J.S., W.G., J.H., W.X., J.D., Q.W., C.-C.L., R.Z., J.C., C.J., J. Zhou, J.B.G., J. Zhu, and Y.Y. analyzed data; X.L. and J. Zhou wrote the paper; and all authors commented on the paper.

Reviewers: A.T., University of Cologne; and X.W., Nanjing University.

The authors declare no conflict of interest.

[1]X.L., D.C., and M.J. contributed equally to this work.

[2]To whom correspondence may be addressed. Email: jgoodenough@mail.utexas.edu, zhujl@sustech.edu.cn, or ygyao@bit.edu.cn.

This article contains supporting information online at www.pnas.org/lookup/suppl/doi:10.1073/pnas.1909276116/-/DCSupplemental.

Published online August 16, 2019.

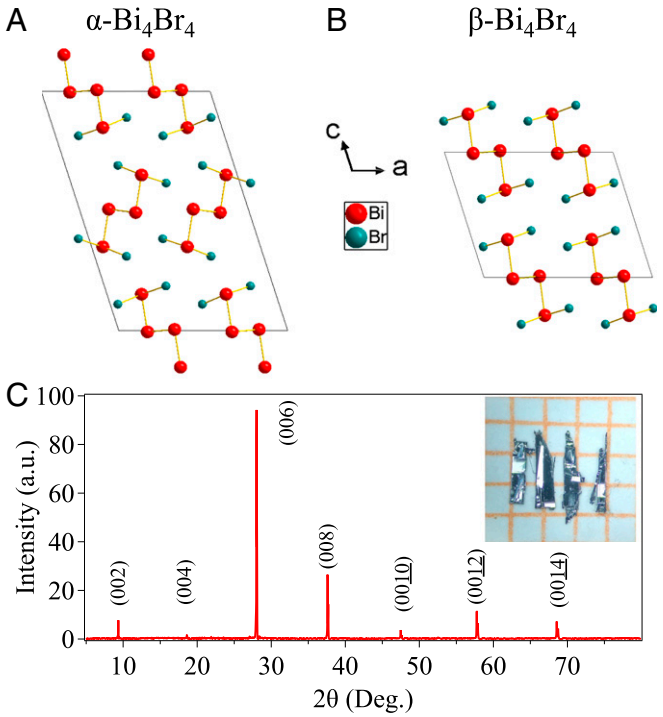

Fig. 1. Quasi-1D crystal structures of (*A*) α-Bi_4Br_4 and (*B*) β-Bi_4Br_4, in which quasi-1D chains run along the *c* axis and stack along the *a* axis via van der Waals interactions. (*C*) PXRD of α-Bi_4Br_4 flakes with the *c* axis coaligned normal to the sample holder under ambient condition. (*Inset*) A picture of a-Bi_4Br_4 crystals on the paper with millimeter grid.

by experiment, the quasi-1D α-Bi_4Br_4 with a different packing of chains is the only stable crystalline phase of Bi_4Br_4 at ambient pressure (23). Its unique symmetry indicator of $Z_{2\times2\times2\times4}$ (0, 0, 0, 2) guarantees that it is not a trivial insulator but a rotation-protected TCI (12). Therefore, it is of interest to see whether pressure can induce topological phases and phenomena in the promising Bi_4Br_4 system. Here, we make a thorough study of Bi_4Br_4 under quasihydrostatic pressure by performing both experimental measurements and theoretical calculations.

Results

Pressure-Induced Insulator–Metal Transition. Needle-shaped single crystals of α-Bi_4Br_4 with dimensions up to 3 × 0.3 × 0.1 mm were grown by a self-flux method. Details can be found in *SI Appendix*. The sample quality was verified by powder X-ray diffraction (PXRD) (Fig. 1*C* and *SI Appendix*, Fig. S1*A*) and energy-dispersive X-ray spectroscopy (EDX) (*SI Appendix*, Fig. S1*B*), which show no sign of any Bi impurity. As illustrated in Fig. 1*A*, the quasi-1D structure of α-Bi_4Br_4 with a strong anisotropy can be easily cleaved along the *ab* plane. The electrical resistance of freshly cleaved α-Bi_4Br_4 crystals was measured in a standard 4-probe configuration under quasihydrostatic pressure (*SI Appendix*, Fig. S2).

Fig. 2*A* shows the electrical resistance as a function of temperature measured under 0 magnetic field in the low-pressure range up to 3.8 GPa. At ambient pressure, the resistance above 200 K shows a semiconductive temperature dependence with a thermal activation energy Δ = 45.7 meV (Fig. 2 *B*, *Inset*), slightly larger than that reported for β-Bi_4I_4 (17). In the pressure range of ∼2.3 to 3.0 GPa, the resistance still shows a semiconductive behavior, but the activation energy becomes smaller (*SI Appendix*, Fig. S3). Intriguingly, there is a steep upturn in ambient pressure resistance that signals a charge density wave (CDW) transition (24). The possible CDW transition temperature T_{CDW} (Fig. 2*B*), which is identified from the maximum of $d(\ln R^*)/d(1/T)$, where $R^* = R(T)/R(300\ \mathrm{K})$, gradually shifts from 23 K at ambient pressure to 6 K at 2.3 GPa and becomes difficult to observe at $P \geq 3.0$ GPa. Further application of pressure gives rise to a metallic character combined with a superconductive transition at low temperatures (Fig. 3*A*, green). It is important to note that the cooldown and warmup resistance curves overlap perfectly below 3.0 GPa, whereas a large resistive hysteresis loop in the temperature interval between 140 and 220 K can be clearly seen at 3.0 GPa in Fig. 2*A*, which was confirmed in a separate run performed on another piece of crystal flake grown in a different batch, indicating a first-order transition. Since the temperature dependences of resistivity above and below the first-order transition are nearly identical, this transition does not seem to be relevant to the insulator–metal transition on crossing a critical pressure $3.0 < P_c < 3.8$ GPa.

Pressure-Induced Superconductivity. An abrupt drop in the resistance at 3.0 GPa emerges at the onset temperature of 6.8 K (Fig. 2*A*, blue) and can be gradually smeared out by an external magnetic field (*SI Appendix*, Fig. S4), indicating filamentary superconductivity. Fig. 3*A* shows the temperature dependence of resistance with pressure up to 45.0 GPa. On lowering the temperature at 3.8 GPa, the 0-field resistance displays a small upturn around 6.8 K, which suggests some change in the electronic ground character, followed by a sharp drop to 0 resistance (Fig. 3*B*). Measurements of the alternating current (AC) susceptibility

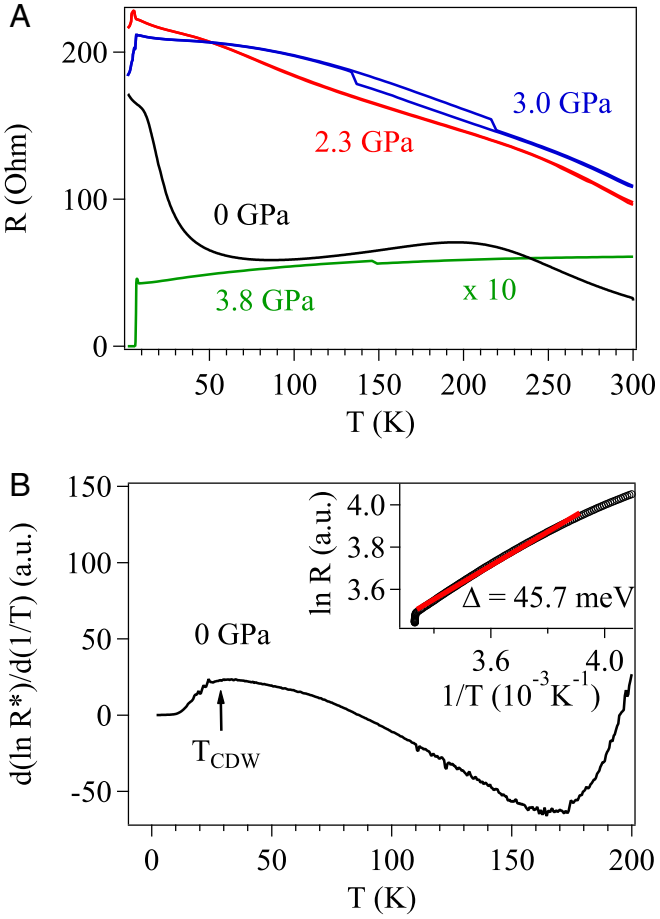

Fig. 2. (*A*) Temperature-dependent resistance of a Bi_4Br_4 crystal under different pressures. (*B*) The derivative resistance of α-Bi_4Br_4 at ambient pressure as a function of temperature. (*Inset*) The resistance of an α-Bi_4Br_4 crystal versus inverse temperature.

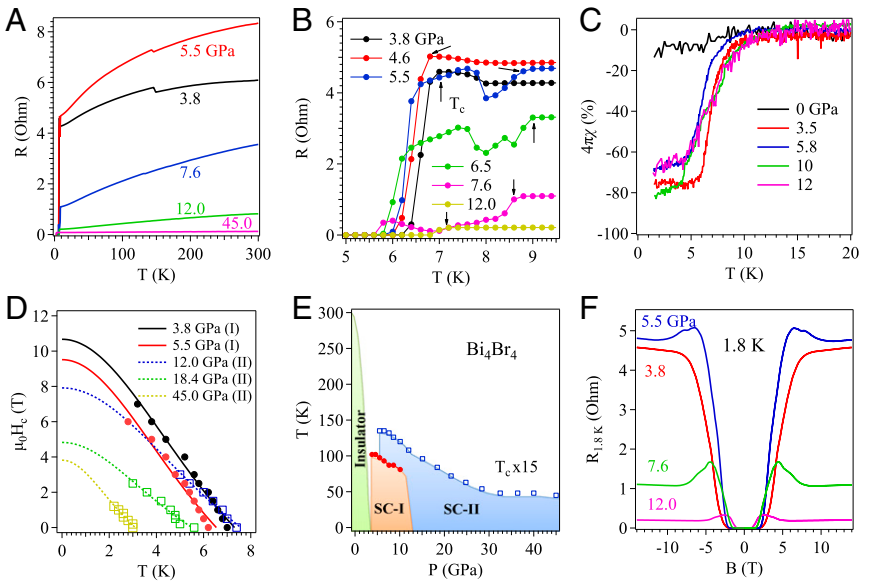

Fig. 3. Temperature dependence of resistance (*A*) at various pressures $P \geq 3.8$ GPa and (*B*) around T_c. (*C*) Temperature dependence of AC magnetic susceptibility up to 10.0 GPa. (*D*) Determination of the upper critical field $\mu_0 H_c(0)$. (*E*) *T*–*P* phase diagram of Bi_4Br_4. (*F*) Magnetic field dependence of resistance of a Bi_4Br_4 crystal at different pressures.

$4\pi\chi$ of the Bi_4Br_4 crystal at various pressures up to 12.0 GPa show clear diamagnetic responses (Fig. 3*C*) (~70 to 80%), confirming a bulk superconductivity. To determine the value of the upper critical magnetic field, $\mu_0 H_c(0)$, we systematically conducted the measurements near the transition temperature under external magnetic fields up to 14 T applied perpendicular to the *ab* plane (*SI Appendix*, Fig. S4). The superconducting transition temperature, T_c, is defined as the temperature where the resistance starts to deviate from the nearly temperature-independent normal-state resistance (these onset temperatures for superconducting transitions are indicated by arrows in Fig. 3*B*). Notably, at each pressure of $P \geq 3.8$ GPa, T_c decreases monotonically with increasing magnetic field, and the upper critical magnetic field $\mu_0 H_c(0)$ can be extrapolated by the Ginzburg–Landau formula $\mu_0 H_c(T) = \mu_0 H_c(0)(1-t^2)/(1+t^2)$, where $t = T/T_c$, as shown in Fig. 3*D*.

As summarized in the temperature-pressure (*T*–*P*) phase diagram shown in Fig. 3*E*, we find that the T_{c1} of the first superconducting (SC-I) phase decreases progressively with pressure and disappears above 12.0 GPa in our measurement, while the T_{c2} of the second superconducting (SC-II) phase appears around 5.5 GPa and manifests a monotonic decrease to the highest pressure 45.0 GPa achieved in the work. The largely different upper critical magnetic fields for the SC-I and SC-II phases indicate their distinct origins of superconductivity. Both of them are smaller than the Bardeen–Cooper–Schrieffer weak-coupling Pauli paramagnetic limit of $1.84T_c$ (12.5*T* at 3.8 GPa for the SC-I phase and 13.2*T* at 12.0 GPa for the SC-II phase). To reveal how the normal state evolves into the superconducting state, we further investigated the magnetic field dependence of magnetoresistance (MR) at various temperatures. In the low-pressure region (*SI Appendix*, Fig. S5), the shape of the nonsaturated positive MR curves in the normal state (e.g., 20 K) changes from a concave curve to a parabolic curve at a critical pressure of 3.8 GPa, where simultaneously, the linear MR curves and bulk superconductivity emerge. At higher pressures, the MR curves in the superconducting state exhibit a U-shaped feature with 2 cusps at a bias field H_{bias} (Fig. 3*F*), which gradually becomes less pronounced as pressure increases. This observation is discussed in detail below.

Pressure-Induced Structural Transition. To clarify whether the superconductive phase transitions are caused by pressure-induced crystal structural transitions, we first conducted an in

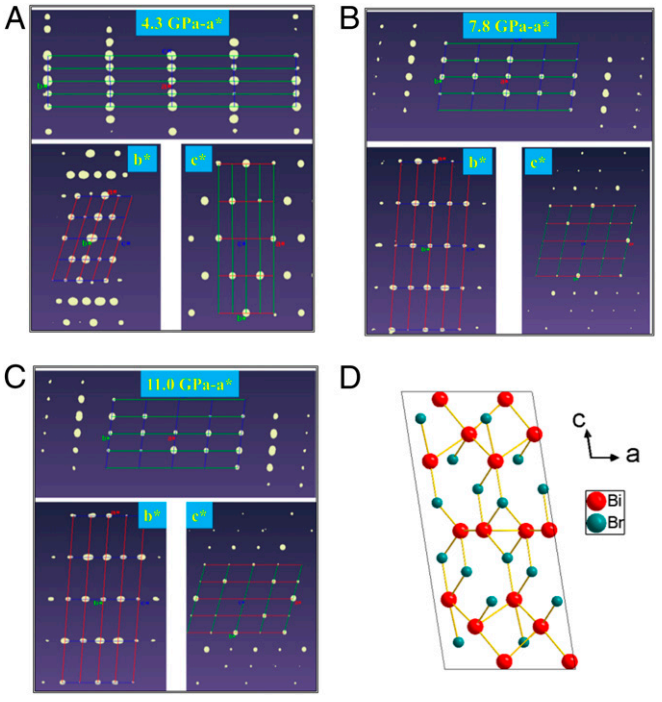

Fig. 4. (*A*) HP-SXRD of Bi_4Br_4 at 4.3 GPa indexed by monoclinic *C*2/*m* structure with lattice parameters of a = 11.254(1) Å, b = 4.454(2) Å, c = 19.085(2) Å, β = 106.22(7)°, and V = 918(1) Å^3. (*B*) HP-SXRD of Bi_4Br_4 at 7.8 GPa indexed by triclinic *P*-1 structure with lattice parameters of a = 5.826(7) Å, b = 8.600(6) Å, c = 18.110(3) Å, α = 97.60(14)°, β = 92.77(18)°, γ = 105.85(8)°, and V = 862(2) Å^3. (*C*) HP-SXRD of Bi_4Br_4 at 11.0 GPa indexed by triclinic *P*-1 structure with lattice parameters of a = 5.685(4) Å, b = 8.498(5) Å, c = 17.830(3) Å, α = 96.92(13)°, β = 92.86(13)°, γ = 104.78(6)°, and V = 824 (2) Å^3. (*D*) Relaxed crystal structure of Bi_4Br_4 at 7.8 GPa.

situ high-pressure single-crystal X-ray diffraction (HP-SXRD) study on an α-Bi_4Br_4 crystal. As shown in Fig. 4*A*, a monoclinic *C*2/*m* structure with lattice parameters of $a = 11.254(1)$ Å, $b = 4.454(2)$ Å, $c = 19.085(2)$ Å, and $\beta = 106.22(7)°$ can be well determined from the collected data at 4.3 GPa, which has the same symmetry as the ambient pressure one but a decrease in the unit cell volume. This observation indicates that the α-Bi_4Br_4 phase is stable against pressure up to 4.3 GPa and that the origin of SC-I superconductivity is independent of a structural phase transition. At 7.8 GPa (Fig. 4*B*), there is a clear change in the crystal symmetry as the crystal converts from monoclinic *C*2/*m* to triclinic *P*-1, with a slight decrease along the *c* direction and a sudden collapse occurring in the *ab* plane (detailed atomic positions are in *SI Appendix*, Table S1). Moreover, all reflections remain quite sharp at 11.0 GPa and can be indexed by the identical *P*-1 symmetry (Fig. 4*C*), revealing that the α-Bi_4Br_4 undergoes a structural transition under hydrostatic conditions between 4.3 and 7.8 GPa, where the SC-II superconducting phase arises. Similar pressure-induced structural transitions from *C*2/*m* to *P*-1 symmetry have been reported in a topological material $ZrTe_5$ (25).

To confirm further the high-pressure phase, we also preformed high-pressure powder X-ray diffraction (HP-PXRD) of α-Bi_4Br_4 fine powders. On compression, however, the data quality worsens, and most reflections broaden significantly so that diffraction patterns cannot be refined. For this reason, we used pieces of crystal clusters with different orientations in the HP-PXRD experiment (*SI Appendix*, Fig. S6). The obtained reflection peaks up to 12 GPa are much sharper, although the peak intensity is not suitable for the structural refinement. A clear structural phase transition has been observed between 3.4 and 7.3 GPa, which is in agreement with the HP-SXRD results. The pattern of the high-pressure phase at 7.3 GPa matches qualitatively with the triclinic *P*-1 lattice. More importantly, the original α-Bi_4Br_4 phase is retrieved after releasing the pressure, ruling out the presence of any Bi as a consequence of pressure-induced phase decomposition. In addition, by preforming first principles calculations based on density functional theory (DFT), we simulated the internal atomic positions for the high-pressure phase staring from those of α-Bi_4Br_4 as displayed in Fig. 4*D*, which are consistent with the experimental results.

Discussion

First, to gain more insight on the pressure-induced insulator–metal transition of α-Bi_4Br_4, we performed DFT calculations of the electronic band structures with and without pressure. The results, similar to those in previous reports, show α-Bi_4Br_4 to be a TCI with a band gap ∼0.2 eV at ambient pressure (Fig. 5 *A* and *B*) (12–16). The highly anisotropic features originate from its quasi-1D structure, in which the intrachain coupling is much stronger than the interchain coupling; the anisotropy not only gives rise to a weaker energy dispersion along the Γ-Z(L) direction in the Brillouin zone (BZ) of Fig. 5*A* but also, makes the band structures along the L-I direction more sensitive to pressure. On increasing pressure to 12 GPa, as shown in Fig. 5*C*, the highest 2 valence bands along the L-I direction approach closer to the Fermi level, and eventually, one branch of them crosses the Fermi level and forms a hole pocket. The conservation of electrons suggests that an electron pocket is found near the Γ point (Fig. 5*C*, purple). These small pockets of holes and electrons thereby make the α-Bi_4Br_4 become a semimetal (Fig. 5 *C* and *D*), which is consistent with the vanishing global band gap observed in our measurements (*SI Appendix*, Fig. S7). However, in the whole BZ, there is still a local band gap with the same topological invariants of (0, 0, 0, 2), indicating that no topological transition occurs during the insulator–metal transition.

Second, before we turn to discuss the origin of the discovered superconductivity, a critical matter is whether the superconductivity arises from a Bi impurity. Although the T_c values of the 2 superconducting transitions are very close to those of Bi under

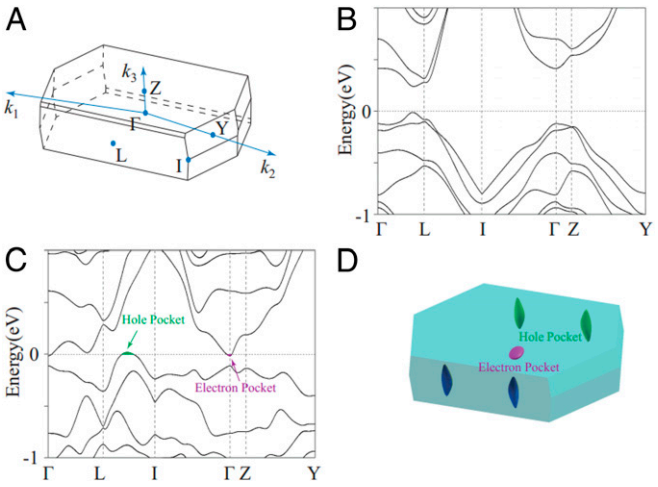

Fig. 5. Electronic band structures of Bi_4Br_4 with and without pressure. (*A*) BZ. (*B*) Band structure at ambient pressure. (*C*) Band structure at 12 GPa. (*D*) Small pockets of holes and electrons forming under high pressure.

pressure (e.g., 6 K at 3 GPa and 8 K at 8 GPa [26]), we have enough evidence to rule out this possibility. 1) As mentioned above, no trace of bulk Bi impurity can be found from PXRD patterns and EDX results in the crystal before loading into the high-pressure device and the crystal recovered from the high-pressure experiment, indicating that the grown crystals are highly phase pure and remain so under high pressure. 2) Both the sharp slope of the superconducting transitions and significant diamagnetic response of the AC susceptibility reveal a bulk effect, certainly not ascribed to a possible filamentary appearance of Bi impurity. 3) If the superconductivity was only stemming from the filaments or the surface, it would be readily suppressed by external magnetic fields. More importantly, the upper critical magnetic fields obtained in Bi_4Br_4 ($\mu_0 H_{c1}$ for the SC-I phase and $\mu_0 H_{c2}$ for the SC-II phase) are much higher than the reported values of 0.1*T* for Bi-II phase and 3.7*T* for Bi-III phase (26), implying that superconductivity in Bi_4Br_4 has nothing to do with any possible Bi decomposed from the sample. 4) The pressure dependence of the T_{c2} of the SC-II phase shows a more pronounced reduction than that of Bi (26). These results, therefore, support that the superconductivity observed in Bi_4Br_4 is mainly intrinsic.

Furthermore, the isostructural topological compound β-Bi_4I_4 exhibits a pressure-induced superconducting transition above 15 GPa (18). Considering that the smaller Br ions in Bi_4Br_4 exert a larger internal chemical pressure on sublattices, it is reasonable to expect that Bi_4Br_4 would become superconducting at a much lower external pressure. Indeed, the SC-I phase with $T_{c1} \sim 6$ K emerges fully at around 3.8 GPa. Meanwhile, our band structure calculations show that the topologically nontrivial features of α-Bi_4Br_4 are protected by its rotational symmetry, which is experimentally identified to be robust against pressure up to 4.3 GPa. It follows that the pressure-induced superconductivity of the SC-I phase might occur in a phase with the nontrivial topology between 3.8 and 4.3 GPa. In contrast, the emergence of superconductivity of the SC-II phase is accompanied by a structural phase transition. A close look at the resistivity of Fig. 3*B* before entering the SC-I phase reveals an anomalous upturn with decreasing temperature, which gradually becomes broader and suppressed together with T_c on applying a magnetic field (*SI Appendix*, Fig. S4). It is also worth noting that the magnetic field dependence of resistivity *R* at 1.8 K (Fig. 3*F*) in the pressure range of ∼5.5 to 12.0 GPa exhibits a cusp-like peak. A similar resistivity upturn in the normal state on cooling and a non-monotonic behavior of MR in an SC phase have been observed

in other low-dimensional disordered superconductors (27–29). These behaviors can be elucidated in terms of phase fluctuations originating from the coexistence of SC and normal-state phases (30, 31). It is very important to note that there is no cusp in the MR at 1.8 K under 3.8 GPa and $P > 12$ GPa. A cusp in the MR has been only observed in the pressure range $5.5 \leq P \geq 12.0$ GPa, where the SC-I and SC-II phases coexist in the phase diagram of Fig. 3*E*. More intriguingly, it is possible to derive a quantum critical point from the residue resistance ratio as a function of pressure, like in black phosphorus under pressure (32) (*SI Appendix*, Fig. S8); a profound change in the electronic structures occurs at $P \sim 19$ GPa.

Conclusions

In conclusion, we performed theoretical calculations and detailed measurements of electrical resistance, AC magnetic susceptibility, and in situ HP-SXRD at various quasihydrostatic pressures on single crystals of α-Bi_4Br_4. A clear insulator–metal transition has been observed between the pressures of 3.0 and 3.8 GPa where the valence and conduction bands cross the Fermi energy at different places in the BZ to form a set of electron and hole pockets. On increasing pressure further, 2 pressure-induced superconducting phases emerge. One of them, the SC-I phase, presents a sharp resistive transition with 0 resistance beginning at 3.8 GPa. Our theoretical calculation demonstrates that the nontrivial topology of α-Bi_4Br_4 persists up to even higher pressure. Consequently, it reveals the possible coexistence of superconductivity and a topologically nontrivial feature protected by the rotational crystal structure symmetry. The SC-II phase coexists with the SC-I phase in the pressure range from 5.5 to 12.0 GPa accompanied by a structural phase transition from the ambient *C*2/*m* phase to a high-pressure *P*-1 phase and further survives with a monotonically decreasing T_c up to 45.0 GPa achieved in this study. These results are crucial for advancing our understanding of the topological quantum phase transitions of Bi_4Br_4.

Materials and Methods

Single crystals of Bi_4Br_4 were grown by self-flux methods. Electronic transport properties of Bi_4Br_4 were measured with a 4-probe electrical conductivity method in a diamond anvil cell (DAC) made of CuBe alloy. HP-SXRD was conducted on a Bi_4Br_4 single crystal with a dimension of $70 \times 40 \times 10$ μm in a DAC. High-pressure AC magnetic susceptibility was measured by using the Palm cubic anvil cell, and the mutual induction method was used (33). Theoretical calculations were performed based on a DFT calculation using the projector-augmented wave method as implemented in the Vienna ab initio simulation package (34). The exchange correlation potential was treated within generalized gradient approximation of Perdew–Burke–Ernzerhof type (35). Detailed information can be found in *SI Appendix*.

ACKNOWLEDGMENTS. This work was supported in part by the National Science Foundation of China Grants 11734003 and U1530402, National Key Research and Development Program of China Grants 2016YFA0300600 and 2016YFA0300904, and Welch Foundation Grant F-1066. J. Zhu was supported by the National Thousand-Young-Talents Program and the National Science Associated Funding Grant U1530402. X.L. was supported by the Beijing Institute of Technology Research Fund Program for Young Scholars. J. Zhou was supported by the NSF through Center for Dynamics and Control of Materials Grant DMR-1720595. J.C. was supported by the Ministry of Science and Technology of China, the National Science Foundation of China, and Chinese Academy of Sciences Grants 2018YFA0305700, 11574377, 11834016, 11874400, XDB25000000, and QYZDB-SSW-SLH013.

1. M. Z. Hasan, C. L. Kane, Colloquium: Topological insulators. *Rev. Mod. Phys.* **82**, 3045 (2010).
2. X.-L. Qi, S.-C. Zhang, Topological insulators and superconductors. *Rev. Mod. Phys.* **83**, 1057 (2011).
3. B. A. Bernevig, T. L. Hughes, *Topological Insulators and Topological Superconductors* (Princeton University Press, 2013).
4. C.-K. Chiu, J. C. Teo, A. P. Schnyder, S. Ryu, Classification of topological quantum matter with symmetries. *Rev. Mod. Phys.* **88**, 035005 (2016).
5. L. Fu, Topological crystalline insulators. *Phys. Rev. Lett.* **106**, 106802 (2011).
6. S. Sasaki *et al*., Topological superconductivity in Cu(x)Bi(2)Se(3). *Phys. Rev. Lett.* **107**, 217001 (2011).
7. Y. Ando, L. Fu, Topological crystalline insulators and topological superconductors: From concepts to materials. *Annu. Rev. Condens. Matter Phys.* **6**, 361–381 (2015).
8. Zhang J *et al*., Pressure-induced superconductivity in topological parent compound Bi_2Te_3. *Proc. Natl. Acad. Sci. U.S.A.* **108**, 24–28 (2011).
9. J. C. Teo, T. L. Hughes, Existence of Majorana-fermion bound states on disclinations and the classification of topological crystalline superconductors in two dimensions. *Phys. Rev. Lett.* **111**, 047006 (2013).
10. Y. Ueno, A. Yamakage, Y. Tanaka, M. Sato, Symmetry-protected Majorana fermions in topological crystalline superconductors: Theory and application to Sr2RuO4. *Phys. Rev. Lett.* **111**, 087002 (2013).
11. F. Zhang, C. L. Kane, E. J. Mele, Topological mirror superconductivity. *Phys. Rev. Lett.* **111**, 056403 (2013).
12. F. Tang, H. C. Po, A. Vishwanath, X. Wan, Efficient topological materials discovery using symmetry indicators. *Nat. Phys.* **15**, 470–476 (2019).
13. C.-H. Hsu *et al*., Purely rotational symmetry-protected topological crystalline insulator α-Bi 4 Br 4. *2D Mater*. **6**, 031004 (2019).
14. J.-J. Zhou, W. Feng, C.-C. Liu, S. Guan, Y. Yao, Large-gap quantum spin Hall insulator in single layer bismuth monobromide Bi4Br4. *Nano Lett.* **14**, 4767–4771 (2014).
15. J.-J. Zhou, W. Feng, G.-B. Liu, Y. Yao, Topological edge states in single-and multi-layer Bi4Br4. *New J. Phys.* **17**, 015004 (2015).
16. C.-C. Liu, J.-J. Zhou, Y. Yao, F. Zhang, Weak topological insulators and composite Weyl semimetals: β-Bi4X4 (X=Br, I). *Phys. Rev. Lett.* **116**, 066801 (2016).
17. A. Pisoni *et al*., Pressure effect and superconductivity in the β– B i 4 I 4 topological insulator. *Phys. Rev. B* **95**, 235149 (2017).
18. Qi Y, *et al*., Pressure-induced superconductivity and topological quantum phase transitions in a quasi-one-dimensional topological insulator: Bi4I4. *npj Quantum Mater.* **3**, 4 (2018).
19. X. Wang *et al*., Pressure-induced structural and electronic transitions in bismuth iodide. *Phys. Rev. B* **98**, 174112 (2018).
20. G. Autès *et al*., A novel quasi-one-dimensional topological insulator in bismuth iodide β-Bi4I4. *Nat. Mater.* **15**, 154–158 (2016).
21. D.-Y. Chen *et al*., Quantum transport properties in single crystals of α– Bi 4 I 4. *Phys. Rev. Mater.* **2**, 114408 (2018).
22. R. Noguchi *et al*., A weak topological insulator state in quasi-one-dimensional bismuth iodide. *Nature* **566**, 518–522 (2019).
23. H. G. von Schnering, H. von Benda, C. Kalveram, Wismutmonojodid BiJ, eine Verbindung mit Bi (O) und Bi (II). *Z. Anorg. Allg. Chem.* **438**, 37–52 (1978).
24. T. Filatova *et al*., Electronic structure, galvanomagnetic and magnetic properties of the bismuth subhalides Bi4I4 and Bi4Br4. *J. Solid State Chem.* **180**, 1103–1109 (2007).
25. Y. Zhou *et al*., Pressure-induced superconductivity in a three-dimensional topological material ZrTe5. *Proc. Natl. Acad. Sci. U.S.A.* **113**, 2904–2909 (2016).
26. Y. Li, E. Wang, X. Zhu, H.-H. Wen, Pressure-induced superconductivity in Bi single crystals. *Phys. Rev. B* **95**, 024510 (2017).
27. M. A. Paalanen, A. F. Hebard, R. R. Ruel, Low-temperature insulating phases of uniformly disordered two-dimensional superconductors. *Phys. Rev. Lett.* **69**, 1604–1607 (1992).
28. G. Sambandamurthy, L. W. Engel, A. Johansson, D. Shahar, Superconductivity-related insulating behavior. *Phys. Rev. Lett.* **92**, 107005 (2004).
29. R. Crane *et al*., Survival of superconducting correlations across the two-dimensional superconductor-insulator transition: A finite-frequency study. *Phys. Rev. B* **75**, 184530 (2007).
30. Y. Dubi, Y. Meir, Y. Avishai, Nature of the superconductor-insulator transition in disordered superconductors. *Nature* **449**, 876–880 (2007).
31. Y. Dubi, Y. Meir, Y. Avishai, Theory of the magnetoresistance of disordered superconducting films. *Phys. Rev. B* **73**, 054509 (2006).
32. Z. J. Xiang *et al*., Pressure-induced electronic transition in black phosphorus. *Phys. Rev. Lett.* **115**, 186403 (2015).
33. J.-G. Cheng *et al*., Integrated-fin gasket for palm cubic-anvil high pressure apparatus. *Rev. Sci. Instrum.* **85**, 093907 (2014).
34. G. Kresse, J. Furthmüller, Efficient iterative schemes for ab initio total-energy calculations using a plane-wave basis set. *Phys. Rev. B Condens. Matter* **54**, 11169–11186 (1996).
35. J. P. Perdew, K. Burke, M. Ernzerhof, Generalized gradient approximation made simple. *Phys. Rev. Lett.* **77**, 3865–3868 (1996).